

1 Microbial decomposition processes and vulnerable Arctic soil organic carbon in the 21st century

2

3

4 Junrong Zha and Qianlai Zhuang

5

6 Department of Earth, Atmospheric, and Planetary Sciences and Department of Agronomy,
7 Purdue University, West Lafayette, IN 47907 USA

8

9 Submitted to: *Biogeoscience*

10 Correspondence to: qzhuang@purdue.edu

11

12

13

14

15

16

17

18

19

20

21

22

23

24

25 **Abstract**

26 **Various levels of representations of biogeochemical processes in current biogeochemistry**
27 **models contribute to a large uncertainty in carbon budget quantification. Here, we present**
28 **an uncertainty analysis with a process-based biogeochemistry model, the Terrestrial**
29 **Ecosystem Model (TEM) that was incorporated with detailed microbial mechanisms.**
30 **Ensemble regional simulations with the new model (MIC-TEM) estimated the carbon**
31 **budget of the Arctic ecosystems is 76.0 ± 114.8 Pg C during the 20th century, -3.1 ± 61.7 Pg C**
32 **under the RCP 2.6 scenario and 94.7 ± 46 Pg C under the RCP 8.5 scenario during the 21st**
33 **century. Positive values indicate the regional carbon sink while negative values are source**
34 **to the atmosphere. Compared to the estimates using a simpler soil decomposition**
35 **algorithm in TEM, the new model estimated that the Arctic terrestrial ecosystems stored 12**
36 **Pg less carbon over the 20th century, 19 Pg C and 30 Pg C less under the RCP 8.5 and RCP**
37 **2.6 scenarios, respectively, during the 21st century. When soil carbon within depths 30 cm,**
38 **100 cm and 300 cm was considered as initial carbon in the 21st century simulations, the**
39 **region was estimated to accumulate 65.4, 88.6, and 109.8 Pg C, respectively, under the RCP**
40 **8.5 scenario. In contrast, under the RCP 2.6 scenario, the region lost 0.7, 2.2, and 3 Pg C,**
41 **respectively, to the atmosphere. We conclude that the future regional carbon budget**
42 **evaluation largely depends on whether or not the adequate microbial activities are**
43 **represented in earth system models and the sizes of soil carbon considered in model**
44 **simulations.**

45

46

47

48 **1. Introduction**

49 Northern high-latitude soils and permafrost contain more than 1,600 Pg carbon (Tarnocai
50 et al., 2009). Climate over this region has warmed in recent decades (Serreze and Francis, 2006)
51 and the increase is 1.5 to 4.5 times the global mean (Holland and Bitz, 2003). Warming-induced
52 changes in carbon cycling are expected to exert large feedbacks to the global climate system
53 (Davidson and Janssens, 2006; Christensen and Christensen, 2007; Oechel et al., 2000).

54 Warming is expected to accelerate soil C loss by increasing soil respiration, but
55 increasing nutrient mineralization, thereby stimulating plant net primary production (NPP)
56 (Mack et al., 2004). Thus, the variation of climate may switch the role of the Arctic system
57 between a C sink and a source if soil C loss overtakes NPP (Davidson et al., 2000; Jobbágy and
58 Jackson, 2000). Process-based biogeochemical models such as TEM (Hayes et al., 2014; Raich
59 and Schlesinger, 1992; McGuire et al., 1992; Zhuang et al., 2001, 2002, 2003, 2010, 2013),
60 Biome-BGC (Running and Coughlan, 1988), CASA (Potter et al., 1993), CENTURY (Parton et
61 al., 1994) and Biosphere Energy Transfer Hydrology scheme (BETHY) (Knorr et al., 2000) have
62 been widely used to quantify the response of carbon dynamics to climatic changes (Todd-Brown
63 et al., 2012). An ensemble of process-based model simulations suggests that arctic ecosystems
64 acted as a sink of atmospheric CO₂ in recent decades (McGuire et al., 2012; Schimel et al., 2013).
65 However, the response of this sink to increasing levels of atmospheric CO₂ and climate change is
66 still uncertain (Todd-Brown et al., 2013). The IPCC 5th report also shows that land carbon
67 storage is the largest source of uncertainty in the global carbon budget quantification (Ciais et al.,
68 2013).

69 Much of the uncertainty is also due to the relatively lower levels of representation of
70 ecosystem processes that determine the exchanges of water, energy and C between land
71 ecosystems and the atmosphere (Wieder et al., 2013), and ignorance of some key biogeochemical
72 mechanisms (Schmidt et al., 2011). For example, heterotrophic respiration (R_H) is the primary
73 loss pathway for soil organic carbon (Hanson et al., 2000; Bond-Lamberty and Thomson, 2010),
74 and it generally increases with increasing temperature (Davidson and Janssens, 2006) and
75 moisture levels in well-drained soils (Cook and Orchard, 2008). Moreover, this process is closely
76 related to soil nitrogen mineralization that determines soil N availability and affects gross
77 primary production (Hao et al., 2015). To date, most models treated soil decomposition as a
78 first-order decay process, i.e., CO_2 respiration is directly proportional to soil organic carbon.
79 However, it is not clear if these models are robust under changing environmental conditions
80 (Lawrence et al., 2011; Schimel and Weintraub, 2003; Barichivich et al., 2013) since they often
81 ignored the effects of changes in biomass and composition of decomposers, while recent
82 empirical studies have shown that microbial abundance and community play a significant role in
83 soil carbon decomposition (Allison and Martiny, 2008). The control that microbial activity and
84 enzymatic kinetics imposed on soil respiration suggests the need for explicit representation of
85 microbial physiology, enzymatic activity, in addition to the direct effects of soil temperature and
86 soil moisture on heterotrophic respiration (Schimel and Weintraub, 2003). Recent
87 mechanistically-based models explicitly incorporated with the microbial dynamics and enzyme
88 kinetics that catalyze soil C decomposition have produced notably different results and a closer
89 match to contemporary observations (Wieder et al., 2013; Allison et al., 2010) indicating the need

90 for incorporating these microbial mechanisms into large-scale earth system models to quantify
91 carbon dynamics under future climatic conditions ((Wieder et al., 2013; Allison et al., 2010).

92 This study advanced a microbe-based biogeochemistry model (MIC-TEM) based on an
93 extant Terrestrial Ecosystem Model (TEM) (Raich and Schlesinger, 1992; McGuire et al., 1992;
94 Zhuang et al., 2001, 2002, 2003, 2010, 2013; Hao et al., 2015). In MIC-TEM, the heterotrophic
95 respiration is not only a function of soil temperature, soil organic matter (SOM) and soil
96 moisture, but also considers the effects of dynamics of microbial biomass and enzyme kinetics
97 (Allison et al., 2010). The verified MIC-TEM was used to quantify the regional carbon dynamics
98 in northern high latitudes (north 45 °N) during the 20th and 21st centuries.

99

100 **2. Methods**

101 **2.1 Overview**

102 Below we first briefly describe how we advanced the MIC-TEM by modifying the soil
103 respiration process in TEM (Zhuang et al., 2003) to better represent carbon dynamics in
104 terrestrial ecosystems. Second, we describe how we parameterized and verified the new model
105 using observed net ecosystem exchange data at representative sites and how simulated net
106 primary productivity (NPP) was evaluated with Moderate Resolution Imaging Spectroradiometer
107 (MODIS) data to demonstrate the reliability of new model at regional scales. Third, we present
108 how we applied the model to the northern high latitudes for the 20th and 21st centuries. Finally,
109 we introduce how we conducted the sensitivity analysis on initial soil carbon input, using
110 gridded observation-based soil carbon data of three soil depths during the 21st century.

111

112 2.2 Model description

113 TEM is a highly aggregated large-scale biogeochemical model that estimates the dynamics of
114 carbon and nitrogen fluxes and pool sizes of plants and soils using spatially-explicit information
115 on climate, elevation, soils and vegetation (McGuire et al., 1992; Zhuang et al., 2003, 2010;
116 Melillo et al., 1993). To explicitly consider the effects of microbial dynamics and enzyme
117 kinetics on large-scale carbon dynamics of northern terrestrial ecosystems, we developed MIC-
118 TEM by coupling version 5.0 of TEM (Zhuang et al., 2003, 2010) with a microbial-enzyme
119 module (Hao et al., 2015; Allison et al., 2010). Our modification of the TEM improved the
120 representation of the heterotrophic respiration (R_H) from a first-order structure to a more detailed
121 structure (Fig. S1).

122 In TEM, heterotrophic respiration R_H is calculated as a function of soil organic carbon
123 (SOC), temperature sensitivity of heterotrophic soil respiration (Q_{10}), soil moisture ($f(\text{MOIST})$),
124 and the gram-specific decomposition constant K_d :

$$125 \quad R_H = K_d * \text{SOC} * Q_{10}^{\frac{\text{temp}}{10}} * f(\text{MOIST}) \quad (1)$$

126 Where temp is soil temperature at top 20 cm (units: °C). CO_2 production from SOC pool is
127 directly proportional to the pool size, and the activity of decomposers only depends on the built-
128 in relationships with soil temperature and moisture (Todd-Brown et al., 2012). Therefore, the
129 changes in microbial community composition or adaption of microbial physiology to new
130 conditions were not represented in TEM. However, current studies indicate that soil C
131 decomposition depends on the activity of biological communities dominated by microbes
132 (Schimel and Weintraub, 2003), implying that the biomass and composition of the decomposer
133 community can't be ignored (Todd-Brown et al., 2012).

134 We thus revised the first-order soil C structure in TEM to a second-order structure
 135 considering microbial dynamics and enzyme kinetics according to Allison et al. (2010). In MIC-
 136 TEM, heterotrophic respiration (R_H) is calculated as:

$$137 \quad R_H = \text{ASSIM} * (1 - \text{CUE}) \quad (2)$$

138 Where ASSIM and CUE represent microbial assimilation and carbon use efficiency, respectively.
 139 ASSIM is modeled with a Michaelis-Menten function:

$$140 \quad \text{ASSIM} = V_{\text{max_uptake}} * \text{MIC} * \frac{\text{DOC}}{K_{\text{m_uptake}} + \text{DOC}} \quad (3)$$

141 Where DOC is dissolved organic carbon and $V_{\text{max_uptake}}$ is the maximum velocity of the
 142 reaction and calculated using the Arrhenius equation:

$$143 \quad V_{\text{max_uptake}} = V_{\text{max_uptake}_0} * e^{\frac{E_{\text{a_uptake}}}{R * (\text{temp} + 273)}} \quad (4)$$

144 Where $V_{\text{max_uptake}_0}$ is the pre-exponential coefficient, $E_{\text{a_uptake}}$ is the activation energy for the
 145 reaction (Jmol^{-1}), R is the gas constant ($8.314 \text{ Jmol}^{-1}\text{K}^{-1}$), and temp is the temperature in Celsius
 146 under the reaction occurs. Here we used soil temperature at top 20 cm.

147 Besides, $K_{\text{m_uptake}}$ is calculated as a linear function of temperature:

$$148 \quad K_{\text{m_uptake}} = K_{\text{m_uptake_slope}} * \text{temp} + K_{\text{m_uptake}_0} \quad (5)$$

149 Microbial biomass MIC is modeled as:

$$150 \quad \frac{d\text{MIC}}{dt} = \text{ASSIM} * \text{CUE} - \text{DEATH} - \text{EPROD} \quad (6)$$

151 Where microbial biomass death (DEATH) and enzyme production (EPROD) are modeled as
 152 proportional to microbial biomass with rate constants r_{death} and r_{EnzProd} :

$$153 \quad \text{DEATH} = r_{\text{death}} * \text{MIC} \quad (7)$$

$$154 \quad \text{EPROD} = r_{\text{EnzProd}} * \text{MIC} \quad (8)$$

155 Where r_{death} and r_{EnzProd} are the rate constants of microbial death and enzyme production,
 156 respectively.

157 DOC is part of soil organic carbon:

$$158 \quad \frac{d\text{DOC}}{dt} = \text{DEATH} * (1 - \text{MICtoSOC}) + \text{DECAY} + \text{ELOSS} - \text{ASSIM} \quad (9)$$

159 Where MICtoSOC is carbon input ratio as dead microbial biomass to SOC, representing the
 160 fraction of microbial death that flows into SOC, and is set as a constant value according to
 161 Allison et al. (2010). SOC dynamics are modeled:

$$162 \quad \frac{d\text{SOC}}{dt} = \text{Litterfall} + \text{DEATH} * \text{MICtoSOC} - \text{DECAY} \quad (10)$$

163 Where Litterfall is estimated as a function of vegetation carbon (Zhuang et al., 2010). The
 164 enzymatic decay of SOC is calculated as:

$$165 \quad \text{DECAY} = V_{\text{max}} * \text{ENZ} * \frac{\text{SOC}}{K_m + \text{SOC}} \quad (11)$$

166 Where V_{max} is the maximum velocity of the reaction and calculated using the Arrhenius equation:

$$167 \quad V_{\text{max}} = V_{\text{max}_0} * e^{\frac{E_a}{R * (\text{temp} + 273)}} \quad (12)$$

168 The parameters K_m and carbon use efficiency (CUE) are temperature sensitive, and calculated
 169 as a linear function of temperature between 0 and 50°C:

$$170 \quad K_m = K_{m_{\text{slope}}} * \text{temp} + K_{m_0} \quad (13)$$

$$171 \quad \text{CUE} = \text{CUE}_{\text{slope}} * \text{temp} + \text{CUE}_0 \quad (14)$$

172 Where $\text{CUE}_{\text{slope}}$ and CUE_0 are parameters for calculating CUE, and $K_{m_{\text{slope}}}$ and K_{m_0} are
 173 parameters for calculating K_m . The values of $\text{CUE}_{\text{slope}}$, CUE_0 , $K_{m_{\text{slope}}}$, and K_{m_0} were derived
 174 from Allison et al. (2010).

175 ELOSS is also a first-order process, representing the loss of enzyme:

176
$$ELOSS = r_{enzloss} * ENZ \quad (15)$$

177 Where $r_{enzloss}$ is the rate constant of enzyme loss. Enzyme pool (ENZ) is modeled:

178
$$\frac{dENZ}{dt} = EPROD - ELOSS \quad (16)$$

179 Heterotrophic respiration (R_H) is an indispensable component of soil respiration (Bond-
180 Lamberty and Thomson, 2010), and closely coupled with soil nitrogen (N) mineralization that
181 determines soil N availability, affecting gross primary production (GPP).

182

183 **2.3 Model parameterization and validation**

184 The variables and parameters of these microbial dynamics and their impacts on soil C
185 decomposition were detailed in Allison et al. (2010) (Table 1). Here we parameterized MIC-
186 TEM for representative ecosystem types in northern high latitudes based on monthly net
187 ecosystem production (NEP, $gCm^{-2} mon^{-1}$) measurements from AmeriFlux network (Davidson et
188 al., 2000) (Table S1). The results for model parameterization were presented in Fig. S2. Another
189 set of level 4 gap-filled NEP data was used for model validation at site level (Table S2). The site-
190 level monthly climate data of air temperature ($^{\circ}C$), precipitation (mm) and cloudiness (%) were
191 used to drive the model. Gridded MODIS NPP data from 2001 to 2010 were used to evaluate
192 regional NPP simulations. The MODIS NPP data was developed by the MOD17 MODIS project.
193 The product name is Net Primary Production Yearly L4 Global 1 km. The critical parameter used
194 in MOD17 algorithm is conversion efficiency parameter ϵ . More information about the MODIS
195 NPP product can be found at
196 https://neo.sci.gsfc.nasa.gov/view.php?datasetId=MOD17A2_M_PSN.

197 In TEM, NPP is calculated as:

198
$$NPP = GPP - R_A \quad (17)$$

199 Where GPP is gross primary production, and R_A is autotrophic respiration. GPP is defined as:

200
$$GPP = C_{max} * f(PAR) * f(phenology) * f(foliage) * f(T) * f(CO_2) * f(NA) * f(FT) \quad (18)$$

201 Where C_{max} is the maximum rate of carbon assimilation, PAR is photosynthetically active
 202 radiation, and $f(phenology)$ represents the effects of leaf area (Raich and Schlesinger, 1992). The
 203 function $f(foliage)$ represents the ratio of canopy leaf biomass relative to maximum leaf biomass
 204 (Zhuang et al., 2002). T is monthly air temperature, and $f(CO_2)$ represents the effects of elevated
 205 atmospheric CO_2 (McGuire et al., 1997; Pan et al., 1998). The function $f(NA)$ models the limiting
 206 effects of plant nitrogen status on GPP (McGuire et al., 1992; Pan et al., 1998). The function f
 207 (FT) represents the effects of freeze-thaw (Zhuang et al., 2003). For detailed GPP and R_A
 208 calculations, see Zhuang et al. (2003).

209 The parameterization was conducted with a global optimization algorithm SCE-UA (Shuffled
 210 complex evolution) (Duan et al., 1994) to minimize the difference between the monthly
 211 simulated and measured NEE at these sites (Fig. S2). The cost function of the minimization is:

212
$$Obj = \sum_{i=1}^k (NEP_{obs,i} - NEP_{sim,i})^2 \quad (19)$$

213 Where $NEP_{obs,i}$ and $NEP_{sim,i}$ are the observed and simulated NEP, respectively. k is the number
 214 of data pairs for comparison. Other parameters used in MIC-TEM were default values from TEM
 215 5.0 (Zhuang et al., 2003, 2010). The optimized parameters were used for model validation and
 216 regional extrapolations.

217

218 **2.4 Regional simulations**

219 Two sets of regional simulations for the 20th century using MIC-TEM and TEM at a spatial
220 resolution of 0.5° latitude × 0.5° longitude were conducted. Gridded forcing data of monthly air
221 temperature, precipitation, and cloudiness were used, along with other ancillary inputs including
222 historical atmospheric CO₂ concentrations, soil texture, elevation, and potential natural
223 vegetation. Climatic inputs vary over time and space, whereas soil texture, elevation, and land
224 cover data are assumed to remain unchanged throughout the 20th century, which only vary
225 spatially. The transient climate data during the 20th century was organized from the Climatic
226 Research Unit (CRU TS3.1) from the University of East Anglia (Harris et al., 2014). The
227 spatially-explicit data include potential natural vegetation (Melillo et al., 1993), soil texture
228 (Zhuang et al., 2003) and elevation (Zhuang et al., 2015).

229 Similarly, two sets of simulations were conducted driven with two contrasting climate
230 change scenarios (RCP 2.6 and RCP 8.5) over the 21st century. The future climate change
231 scenarios were derived from the HadGEM2-ES model, which is a member of CMIP5 project
232 (<https://esgf-node.llnl.gov/search/cmip5/>). The future atmospheric CO₂ concentrations and
233 climate forcing from each of the two climate change scenarios were used. The simulated NPP, R_H
234 and NEP by both models (TEM 5.0 and MIC-TEM) were analyzed. The positive NEP represents
235 a CO₂ sink from the atmosphere to terrestrial ecosystems, while a negative value represents a
236 source of CO₂ from terrestrial ecosystems to the atmosphere.

237 Besides, in order to test the parameter uncertainty in our model, we conducted the
238 regional simulations with 50 sets of parameters for both historical and future studies. The 50 sets
239 of parameters were obtained according to the method in Tang and Zhuang (2008). The upper and
240 lower bounds of the regional estimations were generated based on these simulations.

241

242 **2.5 Sensitivity to initial soil carbon input**

243 Future carbon dynamics can be affected by varying initial soil carbon amount. In the standard
244 simulation of TEM, the initial soil carbon amount for transient simulations was obtained from
245 equilibrium and spin-up periods directly for each grid cell in the region. To test the sensitivity to
246 the initial soil carbon amount in transient simulations for the 21st century, we used empirical soil
247 organic carbon data extracted from the Northern Circumpolar Soil Carbon Database (NCSCD)
248 (Tarnocai et al., 2009), as the initial soil carbon amount. The $0.5^\circ \times 0.5^\circ$ soil carbon data
249 products for three different depths of 30cm, 100cm and 300cm were used. The sensitivity test
250 was conducted for transient simulations under the RCP 2.6 and RCP 8.5 scenarios. To avoid the
251 instability of C-N ratio caused by replacing the initial soil carbon pool with observed data at the
252 beginning of transient period, initial soil nitrogen values were also generated based on the soil
253 carbon data and corresponding C-N ratio map for transient simulations (Zhuang et al., 2003;
254 Raich and Schlesinger, 1992).

255

256 **3. Results**

257 **3.1 Model verification at site and regional levels**

258 With the optimized parameters, MIC-TEM reproduces the carbon dynamics well for alpine
259 tundra, boreal forest, temperate coniferous forest, temperate deciduous forest, grasslands and wet
260 tundra with R^2 ranging from 0.70 for Ivotuk to 0.94 for Bartlett Experimental Forest (Fig. S3,
261 table S3). In general, model performs better for forest ecosystems than for tundra ecosystems.
262 The temporal NPP from 2001 to 2010 simulated by MIC-TEM and TEM were compared with

263 MODIS NPP data (Fig. S4). Pearson correlation coefficients are 0.52 (MIC-TEM and MODIS)
264 and 0.34 (TEM and MODIS). NPP simulated by MIC-TEM showed higher spatial correlation
265 coefficients with MODIS data than TEM (Fig. S5). By considering more detailed microbial
266 activities, the heterotrophic respiration is more adequately simulated using the MIC-TEM. The
267 simulated differences in soil decomposition result in different levels of soil available nitrogen,
268 which influences the nitrogen uptake by plants, the rate of photosynthesis and NPP. The spatial
269 correlation coefficient between NPP simulated by MIC-TEM and MODIS is close to 1 in most
270 study areas, suggesting the reliability of MIC-TEM at the regional scale.

271

272 **3.2 Regional carbon dynamics during the 20th century**

273 The equifinality of the parameters in MIC-TEM was considered in our ensemble regional
274 simulations to measure the parameter uncertainty (Tang and Zhuang, 2008). Here and below, the
275 ensemble means and the inter-simulation standard deviations are shown for uncertainty measure,
276 unless specified as others. These ensemble simulations indicated that the northern high latitudes
277 act from a carbon source of 38.9 Pg C to a carbon sink of 190.8 Pg C by different ensemble
278 members, with the mean of 64.2 ± 21.4 Pg at the end of 20th century while the simulation with the
279 optimized parameters estimates a regional carbon sink of 77.6 Pg with the interannual standard
280 deviation of $0.21 \text{ Pg C yr}^{-1}$ during the 20th century (Fig 1). Simulated regional NEP with
281 optimized parameters using TEM and MIC-TEM showed an increasing trend throughout the 20th
282 century except a slight decrease during the 1960s (Fig. 2). The Spatial distributions of NEP
283 simulated by MIC-TEM for different periods in the 20th century also show the increasing trend
284 (Fig 3). Positive values of NEP represent sinks of CO₂ into terrestrial ecosystems, while negative

285 values represent sources of CO₂ to the atmosphere. From 1900 onwards, both models estimated a
286 regional carbon sink during the 20th century. With optimized parameters, TEM estimated higher
287 NPP and R_H at 0.6 PgC yr⁻¹ and 0.3 PgC yr⁻¹ than MIC-TEM, respectively, at the end of the 20th
288 century (Fig. 2). The MIC-TEM estimated a carbon sink increase from 0.64 to 0.83 PgCyr⁻¹
289 during the century while the estimated increase by TEM was much higher (0.28 PgCyr⁻¹) (Fig. 2).
290 At the end of the century, MIC-TEM estimated NEP reached 1.0 PgCyr⁻¹ in comparison with
291 TEM estimates of 0.3 PgCyr⁻¹. TEM estimated NPP and R_H are 0.5 Pg C yr⁻¹ and 0.3 Pg C yr⁻¹
292 higher, respectively. As a result, TEM estimated that the region accumulated 11.4 Pg more
293 carbon than MIC-TEM. Boreal forests are a major carbon sink at 0.55 and 0.63 Pg C yr⁻¹
294 estimated by MIC-TEM and TEM, respectively. Alpine tundra contributes the least sink. Overall,
295 TEM overestimated the sink by 12.5% in comparison to MIC-TEM for forest ecosystems and
296 16.7% for grasslands. For wet tundra and alpine tundra, TEM overestimated about 20% and 33%
297 in comparison with MIC-TEM, respectively (Table 2).

298

299 **3.3 Regional carbon dynamics during the 21st century**

300 Simulated regional annual NPP and R_H increases under the RCP 8.5 scenario with both models
301 (Fig. 4). With optimized parameters, MIC-TEM estimated NPP increases from 9.2 in the 2000s
302 to 13.2 PgCyr⁻¹ in the 2090s, while TEM-predicted NPP is 2.0 Pg C yr⁻¹ higher in the 2000s and
303 0.3 Pg C yr⁻¹ higher in the 2090s (Fig. 4). Similarly, TEM also overestimated R_H by 1.7 Pg C yr⁻¹
304 in the 2000s and 0.25 Pg C yr⁻¹ higher in the 2090s, respectively (Fig. 4). As a result, the regional
305 sink increases from 0.53 Pg C yr⁻¹ in the 2000s, 1.4 Pg C yr⁻¹ in the 2070s, then decreases to 1.1
306 Pg C yr⁻¹ in the 2090s estimated by MIC-TEM (Fig. 4). Given the uncertainty in parameters,

307 MIC-TEM predicted the region acts as a carbon sink ranging from 48.7 to 140.7 Pg, with the
308 mean of 71.7 ± 26.6 Pg at the end of 21st century, while the simulation with optimized parameters
309 estimates a regional carbon source of 79.5 Pg with the interannual standard deviation of 0.37 Pg
310 C yr⁻¹ during the 21st century (Fig 4). TEM predicted a similar trend for NEP, which
311 overestimated the carbon sink with magnitude of 19.2 Pg compared with the simulation by MIC-
312 TEM with optimized parameters. Under the RCP 2.6 scenario (Fig. 4), the increase of NPP and
313 R_H is smaller from 2000 to 2100 compared to the simulation under the RCP 8.5. MIC-TEM
314 predicted that NPP increases from 9.1 to 10.9 Pg C yr⁻¹, TEM estimated 1.6 Pg C yr⁻¹ higher at
315 the beginning and 0.9 Pg C yr⁻¹ higher in the end of the 21st century (Fig. 4). Consequently, MIC-
316 TEM predicted NEP fluctuates between sinks and sources during the century, with a neutral
317 before 2070, and a source between -0.2 - -0.3 Pg C yr⁻¹ after the 2070s. As a result, the region
318 acts as a carbon source of 1.6 Pg C with the interannual standard deviation of 0.24 Pg C yr⁻¹
319 estimated with MIC-TEM and a sink of 27.6 Pg C with the interannual standard deviation of 0.2
320 Pg C yr⁻¹ estimated with TEM during the century (Fig. 4). When considering the uncertainty
321 source of parameters, MIC-TEM predicted the region acts from a carbon source of 64.8 Pg C to a
322 carbon sink of 58.6 Pg C during the century with the mean of -3.3 ± 20.3 Pg at the end of 21st
323 century (Fig 4).

324

325 **3.4 Model sensitivity to initial soil carbon**

326 Under the RCP 2.6, without replacing the initial soil carbon with inventory-based estimates
327 (Tarnocai et al., 2009) in model simulations, TEM estimated that the regional soil organic carbon

328 (SOC) is 604.2 Pg C and accumulates 12.1 Pg C during the 21st century. When using estimated
329 soil carbon (Tarnocai et al., 2009), within depths of 30cm, 100cm and 300cm as initial pools in
330 simulations, TEM predicted that regional SOC is 429.5, 689.3 and 1003.4 Pg C in 2000, and
331 increases by 9.9, 16.0 and 22.8 Pg C at the end of the 21st century, and the regional cumulative
332 carbon sink is 20.4, 34.0, and 48.1 Pg C, respectively during the century. In contrast, using the
333 same inventory-based SOC estimates, MIC-TEM projected that the region acts from a
334 cumulative carbon sink to a source at 0.7, 2.2, and 3.0 Pg C, respectively. Under the RCP 8.5,
335 both models predicted that the region acts as a carbon sink, regardless of the magnitudes of
336 initial soil carbon pools used, with TEM projected sink of 71.7, 120, and 155.6 Pg C and a much
337 smaller cumulative sink of 65.4, 88.6, and 109.8 Pg C estimated with MIC-TEM, respectively
338 (Table 3).

339 **4. Discussion**

340 During the last few decades, a greening accompanying warming and rising atmospheric
341 CO₂ in the northern high latitudes (>45° N) has been documented (McGuire et al., 1995;
342 McGuire and Hobbie, 1997; Chapin and Starfield, 1997; Stow et al., 2004; Callaghan et al., 2005;
343 Tape et al., 2006). The large stocks of carbon contained in the region (Tarnocai et al., 2009) are
344 particularly vulnerable to climate change (Schuur et al., 2008; McGuire et al., 2009). To date, the
345 degree to which the ecosystems may serve as a source or a sink of C in the future are still
346 uncertain (McGuire et al., 2009; Wieder et al., 2013). Therefore, accurate models are essential for
347 predicting carbon–climate feedbacks in the future (Todd-Brown et al., 2013). Our regional
348 simulations indicate the region is currently a carbon sink, which is consistent with many previous
349 studies (White et al., 2000; Houghton et al., 2007), and this sink will grow under the RCP 8.5

350 scenario, but shift to a carbon source under the RCP 2.6 scenario by 2100. MIC-TEM shows a
351 higher correlation between NPP and soil temperature ($R=0.91$) than TEM ($R=0.82$), suggesting
352 that MIC-TEM is more sensitive to environmental changes (Table S4).

353 Our regional estimates of carbon fluxes by MIC-TEM are within the uncertainty range
354 from other existing studies. For instance, Zhuang et al. (2003) estimated the region as a sink of
355 0.9 Pg C yr^{-1} in extratropical ecosystems for the 1990s, which is similar to our estimation of 0.83
356 Pg C yr^{-1} by MIC-TEM. White et al. (2000) estimated that, during the 1990s, regional NEP
357 above 50°N region is $0.46 \text{ Pg C yr}^{-1}$ while Qian et al. (2010) estimated that NEP increased from
358 0 to 0.3 Pg C yr^{-1} for the high-latitude region above 60°N during last century, and reached 0.25
359 Pg C yr^{-1} during the 1990s. White et al. (2000) predicted that, from 1850 to 2100, the region
360 accumulated 134 Pg C in terrestrial ecosystems, in comparison with our estimates of 77.6 Pg C
361 with MIC-TEM and 89 Pg C with TEM. Our projection of a weakening sink during the second
362 half of the 21st century is consistent with previous model studies (Schaphoff et al., 2013). Our
363 predicted trend of NEP is very similar to the finding of White et al. (2000), indicating that NEP
364 increases from $0.46 \text{ Pg C yr}^{-1}$ in the 2000s and reaches 1.5 Pg C yr^{-1} in the 2070s, then decreases
365 to 0.6 Pg C yr^{-1} in the 2090s.

366 The MIC-TEM simulated NEP generally agrees with the observations. However, model
367 simulations still deviate from the observed data, especially for tundra ecosystems. The deviation
368 may be due to the uncertainty or errors in the observed data, which do not well constrain the
369 model parameters. Uncertain driving data such as temperature and precipitation are also a source
370 of uncertainty for transient simulations. In addition, we assumed that vegetation will not change
371 during the transient simulation. However, over the past few decades in the northern high latitudes,

372 temperature increases have led to vegetation changes (Hansen et al., 2006), including latitudinal
373 treeline advance (Lloyd et al., 2005) and increasing shrub density (Sturm et al., 2001). Vegetation
374 can shift from one type to another because of competition for light, N and water (White et al.,
375 2000). For example, needleleaved trees tend to replace tundra gradually in response to warming.
376 In some areas, forests even moved several hundreds of kilometers within 100 years (Gear and
377 Huntley, 1991). The vegetation changes will affect carbon cycling in these ecosystems. In
378 addition, we have not yet considered the effects of management of agriculture lands (Cole et al.,
379 1997), but Zhuang et al. (2003) showed that the changes in agricultural land use in northern high
380 latitudes have been small.

381 The largest limitation to this study is that we have not explicitly considered the fire
382 effects. Warming in the northern high latitudes could favor fire in its frequency, intensity,
383 seasonality and extent (Kasischke and Turetsky, 2006; Johnstone and Kasischke, 2005; Soja et al.,
384 2007; Randerson et al., 2006; Bond-Lamberty et al., 2007). Fire has profound effects on northern
385 forest ecosystems, altering the N cycle and water and energy exchanges between the atmosphere
386 and ecosystems. Increase in wildfires will destroy most of above-ground biomass and consume
387 organic soils, resulting in less carbon uptake by vegetation (Harden et al., 2000), leading to a net
388 release of carbon in a short term. However, a suite of biophysical mechanisms of ecosystems
389 including post-fire increase in the surface albedo and rates of biomass accumulation may in turn,
390 exert a negative feedback to climate warming (Amiro et al., 2006; Goetz et al., 2007), further
391 influence the carbon exchanges between ecosystems and the atmosphere.

392 Moreover, carbon uptake in land ecosystems depends on new plant growth, which
393 connects tightly with the availability of nutrients such as mineral nitrogen. Recent studies have

394 shown that when soil nitrogen is in short supply, most terrestrial plants would form symbiosis
395 relationships with fungi; hyphae provides nitrogen to plants, in return, plants provide sugar to
396 fungi (Hobbie and Hobbie, 2008, 2006; Schimel and Hättenschwiler, 2007). This symbiosis
397 relationship has not been considered in our current modeling, which may lead to a large
398 uncertainty in our quantification of carbon and nitrogen dynamics.

399 Shift in microbial community structure was not considered in our model, which could
400 affect the temperature sensitivity of heterotrophic respiration (Stone et al., 2012). Michaelis-
401 Menten constant (K_m) could also adapt to climate warming, and it may increase more
402 significantly with increasing temperature in cold-adapted enzymes than in warm-adapted
403 enzymes (German et al., 2012; Somero et al., 2004; Dong and Somero, 2009). Carbon use
404 efficiency (CUE) is also a controversial parameter in our model. Empirical studies in soils
405 suggest that microbial CUE declines by at least $0.009\text{ }^{\circ}\text{C}^{-1}$ (Steinweg et al., 2008), while other
406 studies find that CUE is invariant with temperature (López-Urrutia and Morán, 2007). Another
407 key microbial trait lacking in our modeling is microbial dormancy (He et al., 2015). Dormancy is
408 a common, bet-hedging strategy used by microorganisms when environmental conditions limit
409 their growth and reproduction (Lennon and Jones, 2011). Microorganisms in dormancy are not
410 able to drive biogeochemical processes such as soil CO_2 production, and therefore, only active
411 microorganisms should be involved in utilizing substrates in soils (Blagodatskaya and Kuzyakov,
412 2013). Many studies have indicated that soil respiration responses to environmental conditions
413 are more closely associated with the active portion of microbial biomass than total microbial
414 biomass (Hagerty et al., 2014; Schimel and Schaeffer, 2012; Steinweg et al., 2013). Thus, the

415 ignorance of microbial dormancy could fail to distinguish microbes with different physiological
416 states, introducing uncertainties to our carbon estimation.

417 **5. Conclusions**

418 This study used a more detailed microbial biogeochemistry model to investigate the carbon
419 dynamics in the region for the past and this century. Regional simulations using MIC-TEM
420 indicated that, over the 20th century, the region is a sink of 77.6 Pg C. This sink could reach to
421 79.5 Pg C under the RCP 8.5 scenario or shift to a carbon source of 1.6 Pg under the RCP 2.6
422 scenario during the 21st century. On the other hand, traditional TEM overestimated the carbon
423 sink under the RCP 8.5 scenario with magnitude of 19.2 Pg than MIC-TEM, and predicted this
424 region acting as a carbon sink with magnitude of 27.6 Pg under the RCP 2.6 scenario during the
425 21st century. Using recent soil carbon stock data as initial soil carbon in model simulations, the
426 region was estimated to shift from a carbon sink to a source, with total carbon release at 0.7- 3
427 Pg by 2100 depending on initial soil carbon pools at different soil depths under the RCP 2.6
428 scenario. In contrast, the region acts as a carbon sink at 55.4 - 99.8 Pg in the 21st century under
429 the RCP 8.5 scenario. Without considering more detailed microbial processes, models estimated
430 that the region acts as a carbon sink under both scenarios. Under the RCP 2.6 scenario, the
431 cumulative sink ranges from 9.9 to 22.8 Pg C. Under the RCP 8.5 scenario, the cumulative sink
432 is even larger at 71.7 - 155.6 Pg C. This study indicated that more detailed microbial
433 physiology-based biogeochemistry models estimate carbon dynamics very differently from using
434 a relatively simple microbial decomposition-based model. The comparison with satellite
435 products or other estimates for the 20th century suggests that the more detailed microbial
436 decomposition shall be considered to adequately quantify C dynamics in northern high latitudes.

437 **Acknowledgments**

438 This research was supported by a NSF project (IIS-1027955), a DOE project (DE-SC0008092),
439 and a NASA LCLUC project (NNX09AI26G) to Q. Z. We acknowledge the Rosen High
440 Performance Computing Center at Purdue for computing support. We thank the National Snow
441 and Ice Data center for providing Global Monthly EASE-Grid Snow Water Equivalent data,
442 National Oceanic and Atmospheric Administration for North American Regional Reanalysis
443 (NARR). We also acknowledge the World Climate Research Programme's Working Group on
444 Coupled Modeling Intercomparison Project CMIP5, and we thank the climate modeling groups
445 for producing and making available their model output. The data presented in this paper can be
446 accessed through our research website (<http://www.eaps.purdue.edu/ebdl/>)

447

448 **References**

449 Allison, S. D., and Martiny, J. B.: Colloquium paper: resistance, resilience, and redundancy in
450 microbial communities, *Proceedings of the National Academy of Sciences of the United States*
451 *of America*, 105 Suppl 1, 11512-11519, 10.1073/pnas.0801925105, 2008.
452 Allison, S. D., Wallenstein, M. D., and Bradford, M. A.: Soil-carbon response to warming
453 dependent on microbial physiology, *Nature Geoscience*, 3, 336-340, 10.1038/ngeo846, 2010.
454 Amiro, B. D., Orchansky, A. L., Barr, A. G., Black, T. A., Chambers, S. D., Chapin Iii, F. S.,
455 Goulden, M. L., Litvak, M., Liu, H. P., McCaughey, J. H., McMillan, A., and Randerson, J. T.:
456 The effect of post-fire stand age on the boreal forest energy balance, *Agricultural and Forest*
457 *Meteorology*, 140, 41-50, 10.1016/j.agrformet.2006.02.014, 2006.
458 Barichivich, J., Briffa, K. R., Myneni, R. B., Osborn, T. J., Melvin, T. M., Ciais, P., Piao, S., and
459 Tucker, C.: Large-scale variations in the vegetation growing season and annual cycle of
460 atmospheric CO₂ at high northern latitudes from 1950 to 2011, *Global change biology*, 19, 3167-
461 3183, 10.1111/gcb.12283, 2013.
462 Blagodatskaya, E., and Kuzyakov, Y.: Active microorganisms in soil: Critical review of
463 estimation criteria and approaches, *Soil Biology and Biochemistry*, 67, 192-211,
464 10.1016/j.soilbio.2013.08.024, 2013.
465 Bond-Lamberty, B., Peckham, S. D., Ahl, D. E., and Gower, S. T.: Fire as the dominant driver of
466 central Canadian boreal forest carbon balance, *Nature*, 450, 89-92, 10.1038/nature06272, 2007.

467 Bond-Lamberty, B., and Thomson, A.: Temperature-associated increases in the global soil
468 respiration record, *Nature*, 464, 579-582, 10.1038/nature08930, 2010.

469 Callaghan, T., Björn, L. O., Chernov, Y., Chapin, T., Christensen, T. R., Huntley, B., Ims, R.,
470 Jolly, D., Jonasson, S., Matveyeva, N., Panikov, N., Oechel, W., and Shaver, G.: Arctic tundra
471 and polar desert ecosystems, *Arctic climate impact assessment*, 243-352, 2005.

472 Chapin, F. S., and Starfield, A. M.: Time lags and novel ecosystems in response to transient
473 climatic change in arctic Alaska, *Climatic change*, 35, 449-461, 1997.

474 Christensen, J. H., and Christensen, O. B.: A summary of the PRUDENCE model projections of
475 changes in European climate by the end of this century, *Climatic Change*, 81, 7-30,
476 10.1007/s10584-006-9210-7, 2007.

477 Ciais, P., Sabine, C., Bala, G., Bopp, L., Brovkin, V., Canadell, J., Chhabra, A., DeFries, R.,
478 Galloway, J., Heimann, M., Jones, C., Quéré, C. L., Myneni, R. B., Piao, S., and Thornton, P.:
479 Carbon and other biogeochemical cycles, *Climate change 2013: the physical science basis*.
480 Contribution of Working Group I to the Fifth Assessment Report of the Intergovernmental Panel
481 on Climate Change, 465-570, 2014.

482 Cole, C. V., Duxbury, J., Freney, J., Heinemeyer, O., K. Minami, Mosier, A., Paustian, K.,
483 Rosenberg, N., Sampson, N., Sauerbeck, D., and Zhao, Q.: Global estimates of potential
484 mitigation of greenhouse gas emissions by agriculture, *Nutrient cycling in Agroecosystems*, 49,
485 221-228, 1997.

486 Davidson, E. A., Trumbore, S. E., and Amundson, R.: Biogeochemistry: soil warming and
487 organic carbon content, *Nature*, 408, 2000.

488 Davidson, E. A., and Janssens, I. A.: Temperature sensitivity of soil carbon decomposition and
489 feedbacks to climate change, *Nature*, 440, 165-173, 10.1038/nature04514, 2006.

490 Dong, Y., and Somero, G. N.: Temperature adaptation of cytosolic malate dehydrogenases of
491 limpets (genus *Lottia*): differences in stability and function due to minor changes in sequence
492 correlate with biogeographic and vertical distributions, *The Journal of experimental biology*, 212,
493 169-177, 10.1242/jeb.024505, 2009.

494 Duan, Q., Sorooshian, S., and Gupta, V. K.: Optimal use of the SCE-UA global optimization
495 method for calibrating watershed models, *Journal of Hydrology*, 158, 265-284, 1994.

496 Esteban G. Jobbágy, and Jackson, R. B.: The vertical distribution of soil organic carbon and its
497 relation to climate and vegetation, *Ecological applications*, 10, 423-436, 2000.

498 Gear, A. J., and Huntley, B.: Rapid changes in the range limits of Scots pine 4000 years ago,
499 *Science*, 251, 544-547, 1991.

500 German, D. P., Marcelo, K. R. B., Stone, M. M., and Allison, S. D.: The Michaelis-Menten
501 kinetics of soil extracellular enzymes in response to temperature: a cross-latitudinal study,
502 *Global change biology*, 18, 1468-1479, 10.1111/j.1365-2486.2011.02615.x, 2012.

503 Goetz, S. J., Mack, M. C., Gurney, K. R., Randerson, J. T., and Houghton, R. A.: Ecosystem
504 responses to recent climate change and fire disturbance at northern high latitudes: observations
505 and model results contrasting northern Eurasia and North America, *Environmental Research*
506 *Letters*, 2, 045031, 10.1088/1748-9326/2/4/045031, 2007.

507 Hagerty, S. B., van Groenigen, K. J., Allison, S. D., Hungate, B. A., Schwartz, E., Koch, G. W.,
508 Kolka, R. K., and Dijkstra, P.: Accelerated microbial turnover but constant growth efficiency
509 with warming in soil, *Nature Climate Change*, 4, 903-906, 10.1038/nclimate2361, 2014.

510 Hansen, J., Sato, M., Ruedy, R., Lo, K., Lea, D. W., and Medina-Elizade, M.: Global
511 temperature change, *Proceedings of the National Academy of Sciences of the United States of*
512 *America*, 103, 14288-14293, 10.1073/pnas.0606291103, 2006.

513 Hanson, P. J., Edwards, N. T., Garten, C. T., and Andrews, J. A.: Separating root and soil
514 microbial contributions to soil respiration: A review of methods and observations,
515 *Biogeochemistry*, 48, 115-146, 2000.

516 Hao, G., Zhuang, Q., Zhu, Q., He, Y., Jin, Z., and Shen, W.: Quantifying microbial
517 ecophysiological effects on the carbon fluxes of forest ecosystems over the conterminous United
518 States, *Climatic Change*, 133, 695-708, 10.1007/s10584-015-1490-3, 2015.

519 Harden, J. W., Trumbore, S. E., Stocks, B. J., Hirsch, A., Gower, S. T., O'Neill, K. P., and
520 Kasischke, E. S.: The role of fire in the boreal carbon budget, *Global change biology*, 6, 174-184,
521 2000.

522 Harris, I., Jones, P. D., Osborn, T. J., and Lister, D. H.: Updated high-resolution grids of monthly
523 climatic observations - the CRU TS3.10 Dataset, *International Journal of Climatology*, 34, 623-
524 642, 10.1002/joc.3711, 2014.

525 Hayes, D. J., Kicklighter, D. W., McGuire, A. D., Chen, M., Zhuang, Q., Yuan, F., Melillo, J. M.,
526 and Wullschleger, S. D.: The impacts of recent permafrost thaw on land-atmosphere greenhouse
527 gas exchange, *Environmental Research Letters*, 9, 045005, 10.1088/1748-9326/9/4/045005, 2014.

528 He, Y., Yang, J., Zhuang, Q., Harden, J. W., McGuire, A. D., Liu, Y., Wang, G., and Gu, L.:
529 Incorporating microbial dormancy dynamics into soil decomposition models to improve
530 quantification of soil carbon dynamics of northern temperate forests, *Journal of Geophysical*
531 *Research: Biogeosciences*, 120, 2596-2611, 10.1002/2015jg003130, 2015.

532 Hobbie, E. A., and Hobbie, J. E.: Natural Abundance of ^{15}N in Nitrogen-Limited Forests and
533 Tundra Can Estimate Nitrogen Cycling Through Mycorrhizal Fungi: A Review, *Ecosystems*, 11,
534 815-830, 10.1007/s10021-008-9159-7, 2008.

535 Hobbie, J. E., and Hobbie, E. A.: ^{15}N in symbiotic fungi and plants estimates nitrogen and
536 carbon flux rates in Arctic tundra, *Ecology*, 87, 816-822, 2006.

537 Holland, M. M., and Bitz, C. M.: Polar amplification of climate change in coupled models,
538 *Climate Dynamics*, 21, 221-232, 10.1007/s00382-003-0332-6, 2003.

539 Houghton, R. A.: Balancing the Global Carbon Budget, *Annual Review of Earth and Planetary*
540 *Sciences*, 35, 313-347, 10.1146/annurev.earth.35.031306.140057, 2007.

541 Johnstone, J. F., and Kasischke, E. S.: Stand-level effects of soil burn severity on postfire
542 regeneration in a recently burned black spruce forest, *Canadian Journal of Forest Research*, 35,
543 2151-2163, 10.1139/x05-087, 2005.

544 Kasischke, E. S., and Turetsky, M. R.: Recent changes in the fire regime across the North
545 American boreal region—Spatial and temporal patterns of burning across Canada and Alaska,
546 *Geophysical Research Letters*, 33, 10.1029/2006gl025677, 2006.

547 Knorr, W.: Annual and interannual CO_2 exchanges of the terrestrial biosphere: process-based
548 simulations and uncertainties, *Global Ecology and Biogeography*, 9, 225-252, 2000.

549 Lawrence, D. M., Oleson, K. W., Flanner, M. G., Thornton, P. E., Swenson, S. C., Lawrence, P.
550 J., Zeng, X., Yang, Z.-L., Levis, S., Sakaguchi, K., Bonan, G. B., and Slater, A. G.:
551 Parameterization improvements and functional and structural advances in Version 4 of the
552 Community Land Model, *Journal of Advances in Modeling Earth Systems*, 3,
553 10.1029/2011ms000045, 2011.

554 Lennon, J. T., and Jones, S. E.: Microbial seed banks: the ecological and evolutionary
555 implications of dormancy, *Nature reviews. Microbiology*, 9, 119-130, 10.1038/nrmicro2504,
556 2011.

557 Lloyd, A. H.: Ecological histories from Alaskan tree lines provide insight into future change,
558 *Ecology*, 86, 1687-1695, 2005.

559 Mack, M. C., Schuur, E. A. G., Bret-Harte, M. S., Shaver, G. R., and III, F. S. C.: Ecosystem
560 carbon storage in arctic tundra reduced by long-term nutrient fertilization, *Nature*, 431, 2004.

561 McGuire, A. D., Melillo, J. M., Joyce, L. A., Kicklighter, D. W., Grace, A. L., III, B. M., and
562 Vorosmarty, C. J.: Interactions between carbon and nitrogen dynamics in estimating net primary
563 productivity for potential vegetation in North America, *Global Biogeochemical Cycles*, 6, 101-
564 124, 1992.

565 McGuire, A. D., Melillo, J. M., Kicklighter, D. W., and Joyce, L. A.: Equilibrium responses of
566 soil carbon to climate change: Empirical and process-based estimates, *Journal of Biogeography*,
567 785-796, 1995.

568 McGuire, A. D., and Hobbie, J. E.: Global climate change and the equilibrium responses of
569 carbon storage in arctic and subarctic regions, In *Modeling the Arctic system: A workshop report
570 on the state of modeling in the Arctic System Science program*, 53-54, 1997.

571 McGuire, A. D., Anderson, L. G., Christensen, T. R., Dallimore, S., Guo, L., Hayes, D. J.,
572 Heimann, M., Lorenson, T. D., Macdonald, R. W., and Roulet, N.: Sensitivity of the carbon
573 cycle in the Arctic to climate change, *Ecological Monographs*, 79, 523-555, 2009.

574 McGuire, A. D., Christensen, T. R., Hayes, D., Heroult, A., Euskirchen, E., Kimball, J. S.,
575 Koven, C., Lafleur, P., Miller, P. A., Oechel, W., Peylin, P., Williams, M., and Yi, Y.: An
576 assessment of the carbon balance of Arctic tundra: comparisons among observations, process
577 models, and atmospheric inversions, *Biogeosciences*, 9, 3185-3204, 10.5194/bg-9-3185-2012,
578 2012.

579 Melillo, J. M., McGuire, A. D., Kicklighter, D. W., III, B. M., Vorosmarty, C. J., and Schloss, A.
580 L.: Global climate change and terrestrial net primary production, *Nature*, 363, 1993.

581 Oechel, W. C., Vourlitis, G. L., Hastings, S. J., Zulueta, R. C., Hinzman, L., and Kane, D.:
582 Acclimation of ecosystem CO₂ exchange in the Alaskan Arctic in response to decadal climate
583 warming, *Nature*, 406, 978, 2000.

584 Orchard, V. A., and Cook, F. J.: Relationship between soil respiration and soil moisture, 15, 447-
585 453, 1983.

586 Parton, W. J., Ojima, D. S., Cole, C. V., and Schimel, D. S.: A general model for soil organic
587 matter dynamics: sensitivity to litter chemistry, texture and management, *Quantitative modeling
588 of soil forming processes*, 147-167, 1994.

589 Potter, C. S., Randerson, J. T., Field, C. B., Matson, P. A., Vitousek, P. M., Mooney, H. A., and
590 Klooster, S. A.: Terrestrial ecosystem production: a process model based on global satellite and
591 surface data, *Global Biogeochemical Cycles*, 7, 811-841, 1993.

592 Qian, H., Joseph, R., and Zeng, N.: Enhanced terrestrial carbon uptake in the Northern High
593 Latitudes in the 21st century from the Coupled Carbon Cycle Climate Model Intercomparison
594 Project model projections, *Global change biology*, 16, 641-656, 10.1111/j.1365-
595 2486.2009.01989.x, 2010.

596 Raich, J. W., and Schlesinger, W. H.: The global carbon dioxide flux in soil respiration and its
597 relationship to vegetation and climate, *Tellus B*, 44, 81-99, 1992.

598 Randerson, J. T., Liu, H., Flanner, M. G., Chambers, S. D., Jin, Y., Hess, P. G., Pfister, G., Mack,
599 M. C., Treseder, K. K., Welp, L. R., Chapin, F. S., Harden, J. W., Goulden, M. L., Lyons, E.,
600 Neff, J. C., Schuur, E. A. G., and Zender, C. S.: The impact of boreal forest fire on climate
601 warming, *science*, 1130-1132, 2006.

602 Running, S. W., and Coughlan, J. C.: A general model of forest ecosystem processes for regional
603 applications I. Hydrologic balance, canopy gas exchange and primary production processes.,
604 *Ecological Modelling*, 42, 125-154, 1988.

605 Schaphoff, S., Heyder, U., Ostberg, S., Gerten, D., Heinke, J., and Lucht, W.: Contribution of
606 permafrost soils to the global carbon budget, *Environmental Research Letters*, 8, 014026,
607 10.1088/1748-9326/8/1/014026, 2013.

608 Schimel, J.: The implications of exoenzyme activity on microbial carbon and nitrogen limitation
609 in soil: a theoretical model, *Soil Biology and Biochemistry*, 35, 549-563, 10.1016/s0038-
610 0717(03)00015-4, 2003.

611 Schimel, J.: Microbes and global carbon, *Nature Climate Change*, 3, 867-868,
612 10.1038/nclimate2015, 2013.

613 Schimel, J. P., and Hättenschwiler, S.: Nitrogen transfer between decomposing leaves of
614 different N status, *Soil Biology and Biochemistry*, 39, 1428-1436, 10.1016/j.soilbio.2006.12.037,
615 2007.

616 Schimel, J. P., and Schaeffer, S. M.: Microbial control over carbon cycling in soil, *Frontiers in*
617 *microbiology*, 3, 348, 10.3389/fmicb.2012.00348, 2012.

618 Schmidt, M. W., Torn, M. S., Abiven, S., Dittmar, T., Guggenberger, G., Janssens, I. A., Kleber,
619 M., Kogel-Knabner, I., Lehmann, J., Manning, D. A., Nannipieri, P., Rasse, D. P., Weiner, S.,
620 and Trumbore, S. E.: Persistence of soil organic matter as an ecosystem property, *Nature*, 478,
621 49-56, 10.1038/nature10386, 2011.

622 Schuur, E. A. G., Bockheim, J., Canadell, J. G., Euskirchen, E., Field, C. B., Goryachkin, S. V.,
623 Hagemann, S., Kuhry, P., Lafleur, P. M., Lee, H., and Mazhitova, G.: Vulnerability of
624 permafrost carbon to climate change: Implications for the global carbon cycle, *BioScience*, 58,
625 701-714, 2008.

626 Serreze, M. C., and Francis, J. A.: The Arctic on the fast track of change, *Weather*, 61, 65-69,
627 2006.

628 Soja, A. J., Tchepakova, N. M., French, N. H. F., Flannigan, M. D., Shugart, H. H., Stocks, B. J.,
629 Sukhinin, A. I., Parfenova, E. I., Chapin, F. S., and Stackhouse, P. W.: Climate-induced boreal
630 forest change: Predictions versus current observations, *Global and Planetary Change*, 56, 274-
631 296, 10.1016/j.gloplacha.2006.07.028, 2007.

632 Somero, G. N.: Adaptation of enzymes to temperature: searching for basic "strategies",
633 *Comparative biochemistry and physiology. Part B, Biochemistry & molecular biology*, 139, 321-
634 333, 10.1016/j.cbpc.2004.05.003, 2004.

635 Steinweg, J. M., Plante, A. F., Conant, R. T., Paul, E. A., and Tanaka, D. L.: Patterns of substrate
636 utilization during long-term incubations at different temperatures, *Soil Biology and Biochemistry*,
637 40, 2722-2728, 10.1016/j.soilbio.2008.07.002, 2008.

638 Steinweg, J. M., Dukes, J. S., Paul, E. A., and Wallenstein, M. D.: Microbial responses to multi-
639 factor climate change: effects on soil enzymes, *Frontiers in microbiology*, 4, 146,
640 10.3389/fmicb.2013.00146, 2013.

641 Stone, M. M., Weiss, M. S., Goodale, C. L., Adams, M. B., Fernandez, I. J., German, D. P., and
642 Allison, S. D.: Temperature sensitivity of soil enzyme kinetics under N-fertilization in two
643 temperate forests, *Global change biology*, 18, 1173-1184, 10.1111/j.1365-2486.2011.02545.x,
644 2012.

645 Stow, D. A., Hope, A., McGuire, D., Verbyla, D., Gamon, J., Huemmrich, F., Houston, S.,
646 Racine, C., Sturm, M., Tape, K., Hinzman, L., Yoshikawa, K., Tweedie, C., Noyle, B.,
647 Silapaswan, C., Douglas, D., Griffith, B., Jia, G., Epstein, H., Walker, D., Daeschner, S.,
648 Petersen, A., Zhou, L., and Myneni, R.: Remote sensing of vegetation and land-cover change in
649 Arctic Tundra Ecosystems, *Remote Sensing of Environment*, 89, 281-308,
650 10.1016/j.rse.2003.10.018, 2004.

651 Sturm, M., Racine, C., and Tape, K.: Climate change: increasing shrub abundance in the Arctic.,
652 *Nature*, 411, 2001.

653 Tang, J., and Zhuang, Q.: Equifinality in parameterization of process-based biogeochemistry
654 models: A significant uncertainty source to the estimation of regional carbon dynamics, *Journal*
655 *of Geophysical Research: Biogeosciences*, 113, 10.1029/2008jg000757, 2008.

656 Tape, K. E. N., Sturm, M., and Racine, C.: The evidence for shrub expansion in Northern Alaska
657 and the Pan-Arctic, *Global change biology*, 12, 686-702, 10.1111/j.1365-2486.2006.01128.x,
658 2006.

659 Tarnocai, C., Canadell, J. G., Schuur, E. A. G., Kuhry, P., Mazhitova, G., and Zimov, S.: Soil
660 organic carbon pools in the northern circumpolar permafrost region, *Global Biogeochemical*
661 *Cycles*, 23, n/a-n/a, 10.1029/2008gb003327, 2009.

662 Todd-Brown, K. E. O., Hopkins, F. M., Kivlin, S. N., Talbot, J. M., and Allison, S. D.: A
663 framework for representing microbial decomposition in coupled climate models,
664 *Biogeochemistry*, 109, 19-33, 10.1007/s10533-011-9635-6, 2011.

665 Todd-Brown, K. E. O., Randerson, J. T., Post, W. M., Hoffman, F. M., Tarnocai, C., Schuur, E.
666 A. G., and Allison, S. D.: Causes of variation in soil carbon simulations from CMIP5 Earth
667 system models and comparison with observations, *Biogeosciences*, 10, 1717-1736, 10.5194/bg-
668 10-1717-2013, 2013.

669 White, A., Cannell, M. G. R., and Friend, A. D.: The high-latitude terrestrial carbon sink: a
670 model analysis *Global change biology*, 6, 227-245, 2000.

671 Wieder, W. R., Bonan, G. B., and Allison, S. D.: Global soil carbon projections are improved by
672 modelling microbial processes, *Nature Climate Change*, 3, 909-912, 10.1038/nclimate1951, 2013.

673 Zhuang, Q., Romanovsky, V. E., and McGuire, A. D.: Incorporation of a permafrost model into a
674 large-scale ecosystem model: Evaluation of temporal and spatial scaling issues in simulating soil
675 thermal dynamics, *Journal of Geophysical Research: Atmospheres*, 106, 33649-33670,
676 10.1029/2001jd900151, 2001.

677 Zhuang, Q., McGuire, A. D., O'Neill, K. P., Harden, J. W., Romanovsky, V. E., and Yarie, J.:
678 Modeling soil thermal and carbon dynamics of a fire chronosequence in interior Alaska, *Journal*
679 *of Geophysical Research*, 108, 10.1029/2001jd001244, 2002.

680 Zhuang, Q., He, J., Lu, Y., Ji, L., Xiao, J., and Luo, T.: Carbon dynamics of terrestrial
681 ecosystems on the Tibetan Plateau during the 20th century: an analysis with a process-based
682 biogeochemical model, *Global Ecology and Biogeography*, no-no, 10.1111/j.1466-
683 8238.2010.00559.x, 2010.

684 Zhuang, Q., Chen, M., Xu, K., Tang, J., Saikawa, E., Lu, Y., Melillo, J. M., Prinn, R. G., and
685 McGuire, A. D.: Response of global soil consumption of atmospheric methane to changes in
686 atmospheric climate and nitrogen deposition, *Global Biogeochemical Cycles*, 27, 650-663,
687 10.1002/gbc.20057, 2013.
688 Zhuang, Q., Zhu, X., He, Y., Prigent, C., Melillo, J. M., David McGuire, A., Prinn, R. G., and
689 Kicklighter, D. W.: Influence of changes in wetland inundation extent on net fluxes of carbon
690 dioxide and methane in northern high latitudes from 1993 to 2004, *Environmental Research*
691 *Letters*, 10, 095009, 10.1088/1748-9326/10/9/095009, 2015.
692 Zhuang, Q., McGuire, A. D., Melillo, J. M., Klein, J. S., Dargaville, R. J., Kicklighter, D. W.,
693 Myneni, R. B., Dong, J., Romanovsky, V. E., Harden, J., and Hobbie, J. E.: Carbon cycling in
694 extratropical terrestrial ecosystems of the Northern Hemisphere during the 20th century: a
695 modeling analysis of the influences of soil thermal dynamics, *Tellus B: Chemical and Physical*
696 *Meteorology*, 55, 751-776, 10.3402/tellusb.v55i3.16368, 2003.
697 Zimov, S. A., Schuur, E. A. G., and III, F. S. C.: Permafrost and the global carbon budget,
698 *Science*, 312, 1612-1613, 2006.

699

700

701 **Author contributions.** Q.Z. designed the study. J.Z. conducted model development, simulation
702 and analysis. J.Z. and Q. Z. wrote the paper.

703

704 **Competing financial interests.** The submission has no competing financial interests.

705

706 **Materials & Correspondence.** Correspondence and material requests should be addressed to
707 qzhuang@purdue.edu.

708

709

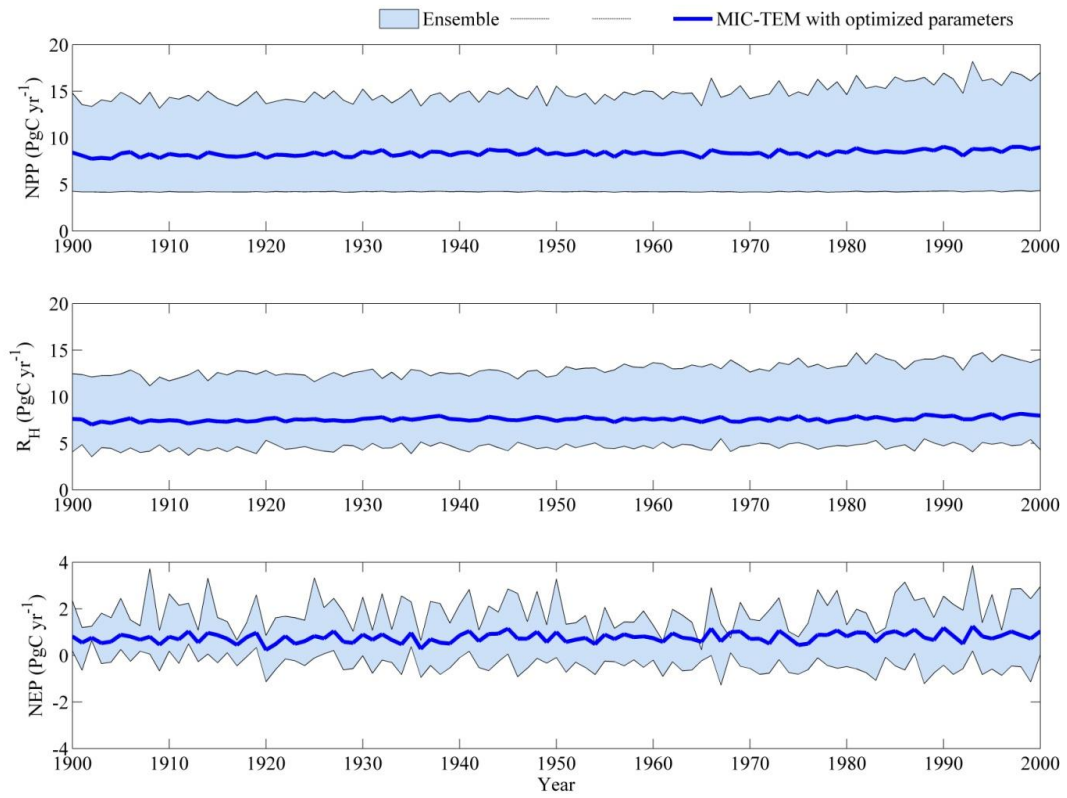


Figure 1. Simulated annual net primary production (NPP, top panel), heterotrophic respiration (R_H , center panel) and net ecosystem production (NEP, bottom panel) by MIC-TEM with ensemble of parameters.

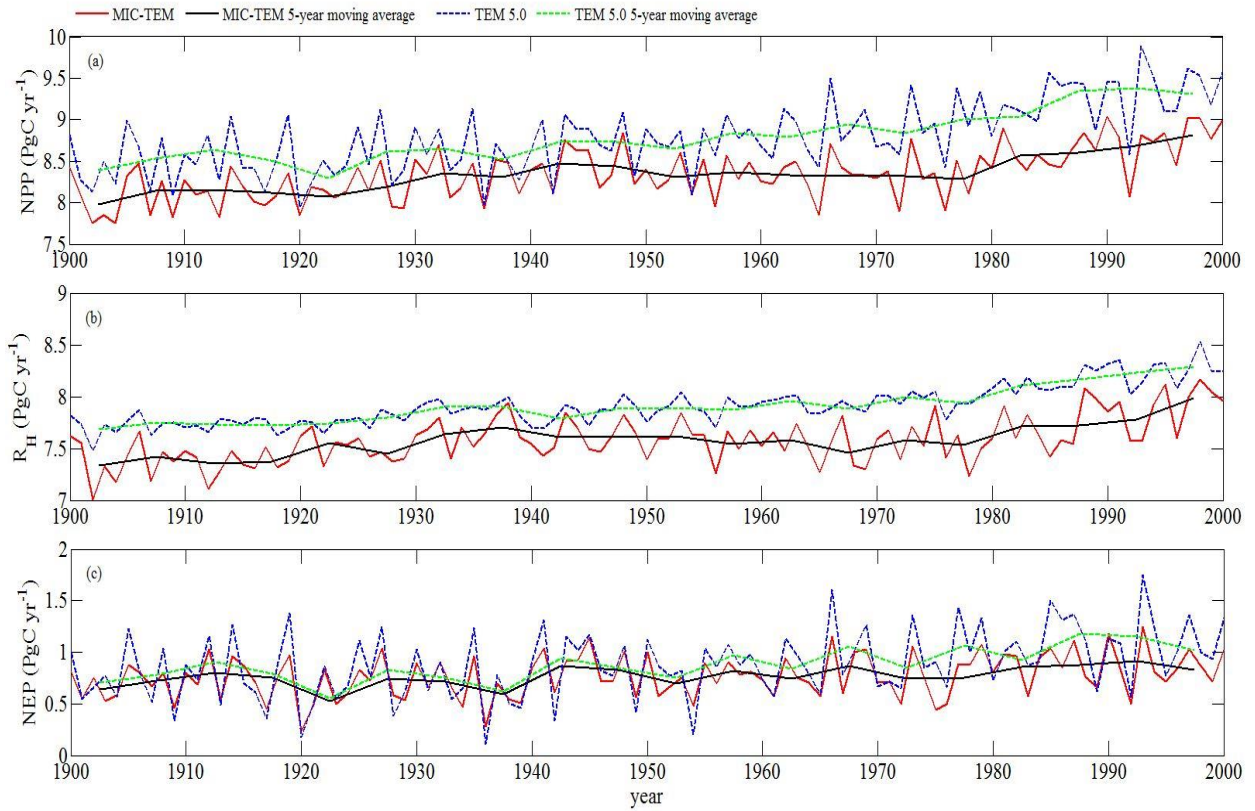


Figure 2. Simulated annual net primary production (NPP, top panel), heterotrophic respiration (R_H , center panel) and net ecosystem production (NEP, bottom panel) by MIC-TEM and TEM, respectively.

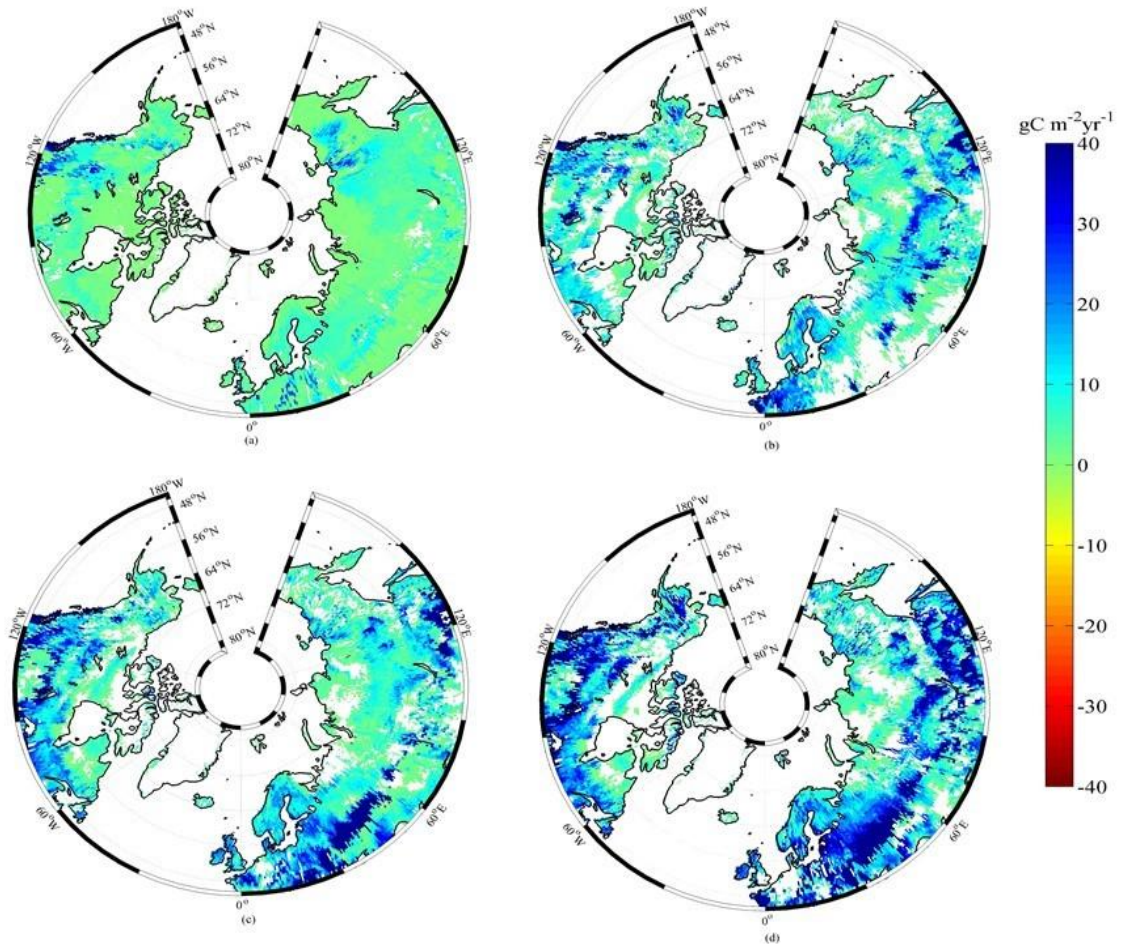


Figure 3. Spatial distribution of NEP simulated by MIC-TEM for the periods: (a) 1900-1930, (b) 1931-1960, (c) 1961-1990, and (d) 1991-2000. Positive values of NEP represent sinks of CO_2 into terrestrial ecosystems, while negative values represent sources of CO_2 to the atmosphere.

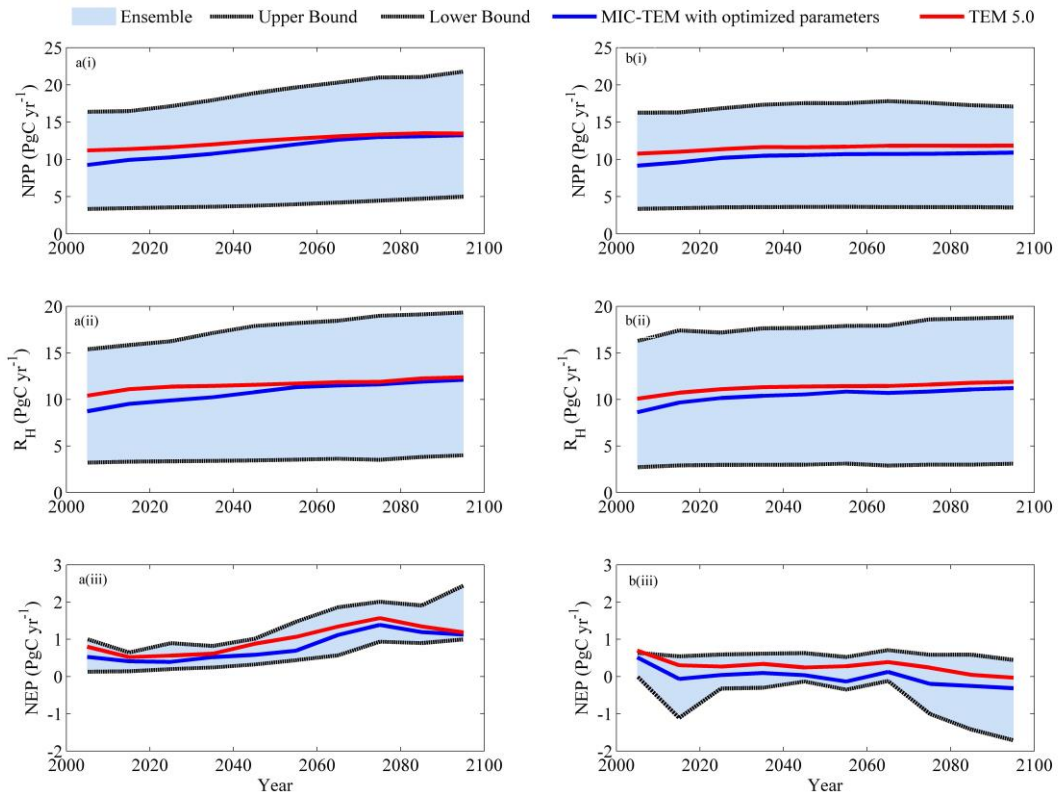


Figure 4. Predicted changes in carbon fluxes: (i) NPP, (ii) R_H , and (iii) NEP for all land areas north of 45°N in response to transient climate change under (a) RCP 8.5 scenario and (b) RCP 2.6 scenario with MIC-TEM and TEM 5.0, respectively. The decadal running mean is applied. The grey area represents the upper and lower bounds of simulations.

Table 1. Parameters associated with more detailed microbial dynamics in MIC-TEM

Process	Parameter	Units	Initial Value	Description	Parameter range	Reference
Assimilation	$Vmax_{uptake_0}$	mg DOC cm ⁻³ (mg biomass cm ⁻³) ⁻¹ h ⁻¹	9.97e6	Maximum microbial uptake rate	[1.0e4, 1.0e8]	Hao et al. (2015)
	Ea_{uptake}	kJ mol ⁻¹	47	Activation energy	-	Allison et al. (2010)
	$Km_{uptake_{slope}}$	mg cm ⁻³ degree ⁻¹	0.01	Temperature regulator of MM for DOC uptake by microbes	-	Allison et al. (2010)
CO ₂ production	Km_{uptake_0}	mg cm ⁻³	0.1	Temperature regulator of MM for DOC uptake by microbes	-	Allison et al. (2010)
	CUE_{slope}	degree ⁻¹	-0.016	Temperature regulator of carbon use efficiency	-	Allison et al. (2010)
	CUE_0	-	0.63	Temperature regulator of carbon use efficiency	-	Allison et al. (2010)
Decay	$Vmax_0$	mg SOC cm ⁻³ (mg Enz cm ⁻³) ⁻¹ h ⁻¹	9.17e7	Maximum rate of converting SOC to soluble C	[1.0e5, 1.0e8]	Hao et al. (2015)
	Ea	kJ mol ⁻¹	47	Activation energy	-	Allison et al. (2010)
	Km_{slope}	mg cm ⁻³ degree ⁻¹	5	Temperature regulator of MM for enzymatic decay	-	Allison et al. (2010)
MIC turnover	Km_0	mg cm ⁻³	500	Temperature regulator of MM for enzymatic decay	-	Allison et al. (2010)
	r_{death}	s ⁻¹	0.02	Microbial death fraction	-	Allison et al. (2010)
	MICtoSOC		50	Partition coefficient for dead microbial biomass between the SOC and DOC pool	-	Allison et al. (2010)
ENZ turnover	$r_{EnzProd}$	s ⁻¹	5.0e-4	Enzyme production fraction	-	Allison et al. (2010)
	$r_{EnzLoss}$	s ⁻¹	0.1	Enzyme loss fraction	-	Allison et al. (2010)

Table 2. Partitioning of average annual net ecosystem production (as Pg C per year) for six vegetation types during the 20th century

	MIC-TEM (PgC yr ⁻¹)	TEM 5.0 (PgC y ⁻¹)
Alpine tundra	0.03	0.04
Boreal forest	0.39	0.45
Conifer forest	0.09	0.09
Deciduous forest	0.16	0.18
Grassland	0.06	0.07
Wet tundra	0.05	0.06
Total	0.78	0.89

Table 3. Increasing of SOC, vegetation carbon (VGC), soil organic nitrogen (SON), vegetation nitrogen (VGN) from 1900 to 2000, and total carbon storage during the 21st century predicted by two models with observed soil carbon data of three different depths under (a) RCP 2.6 and (b) RCP 8.5.

(a)

Model	Units: Pg	Without (control)	30cm	100cm	300cm
TEM 5.0	SOC/SON in 2000	604.2/27.0	429.5/19.0	689.3/31.6	1003.4/46.2
	Increase of SOC during the 21 st century	12.1	9.9	16.0	22.8
	VGC/VGN in 2000	318.3/1.48	238.4/1.05	394.2/1.80	556.7/2.53
	Increase of VGC during the 21 st century	15.5	10.5	18.0	25.3
	Increase of total carbon storage during the 21 st century	27.6	20.4	34.0	48.1
MIC-TEM	SOC/SON in 2000	591.5/26.8	420.3/18.6	686.0/31.2	990.7/45.3
	Increase of SOC during the 21 st century	-2.0	-1.2	-2.4	-2.9
	VGC/VGN in 2000	309.7/1.42	230.1/1.02	374.4/1.71	548.6/2.45
	Increase of VGC during the 21 st century	0.4	0.5	0.2	-0.1
	Increase of total carbon storage during the 21 st century	-1.6	-0.7	-2.2	-3.0

(b)

Model	Units: Pg	Without (control)	30cm	100cm	300cm
TEM 5.0	SOC/SON in 2000	610.2 /27.9	431.9/19.1	693.8/31.8	1007.1/46.4
	Increase of SOC during the 21 st century	44.2	33.0	56.5	74.6
	VGC/VGN in 2000	324.9/1.50	242.1/1.07	399.6/1.83	570.2/2.57
	Increase of VGC during the 21 st century	54.5	38.7	63.5	81.0
	Increase of total carbon storage during the 21 st century	98.7	71.7	120.0	155.6
MIC-TEM	SOC/SON in 2000	596.0/27.1	424.6/18.8	689.1/31.5	995.5/46.1
	Increase of SOC during the 21 st century	33.3	27.4	36.9	42.9
	VGC/VGN in 2000	316.0/1.44	233.5/1.02	380.0/1.72	568.3/2.56
	Increase of VGC during the 21 st century	46.2	37.0	51.7	56.9
	Increase of total carbon storage during the 21 st century	79.5	65.4	88.6	109.8